JOURNAL OF GEOPHYSICAL RESEARCH, SPACE PHYSICS VOL. 74, NO. 19, SEPTEMBER 1, 1969

Cosmic-Ray Electrons between 12 Mev and 1 Gev in 1967

MARTIN H. ISRAEL[1]

California Institute of Technology, Pasadena, California 91109

Observations of cosmic-ray electrons in the energy range of 12 Mev to 1 Gev were made in 1967 in a series of high-altitude balloon flights with a detector consisting of a scintillation-counter telescope, gas Čerenkov counter, and lead-plate spark chamber. Three flights were launched from Fort Churchill, Manitoba, in the summer of 1967, to measure the vertically incident primary electron flux; a fourth flight gave a direct measurement of splash albedo electrons. In April 1967 return albedo electrons were observed on a flight launched from Palestine, Texas. We derive 2σ upper limits for the flux of primary electrons at the top of the atmosphere of 20, 9, and 13 electrons/m² sec ster in the energy intervals 17–57, 57–112, and 112–374 Mev respectively. Between 374 and 1060 Mev we find 16 ± 14 electrons/m² sec ster. Above 100 Mev these results lie significantly below fluxes reported for 1966 by other observers. Comparison between the observed upper limits to the primary flux and a calculation of the flux of galactic secondary electrons indicates an absolute solar modulation of electrons below 300 Mev by at least a factor of 3. We observed splash albedo fluxes of 94 ± 16, 47 ± 11, 27 ± 9, and 2^{+4}_{-2} electrons/m² sec ster in the energy intervals 12–50, 50–100, 100–350, and 350–1000 Mev, respectively, near Fort Churchill, Manitoba. Near Palestine, Texas, we find 60 ± 26 return albedo electrons/m² sec ster between 25 and 65 Mev. At higher energies the observed flux of downward-moving electrons is consistent with being atmospheric secondaries; we give 2σ upper limits to the return albedo flux of 22, 12, and 6 electrons/m² sec ster in the energy intervals of 65–131, 131–411, and 411–1149 Mev, respectively. These return albedo fluxes are significantly lower than corresponding fluxes previously reported by S. D. Verma but are consistent with results of a calculation by C. J. Bland. Comparison between our observations at Fort Churchill and observations at Palestine indicates a significant contribution to the splash albedo flux from primary particles with rigidity below 4.5 Gv.

INTRODUCTION

Since the first direct observations of primary cosmic-ray electrons in 1960 [*Earl*, 1961; *Meyer and Vogt*, 1961], the electron spectrum has been extensively studied at energies above 200 Mev. (Recent measurements in the energy range of 200 Mev to 1 Gev include the observations of *L'Heureux and Meyer* [1968], *Webber* [1968], *Fanselow* [1968], and *Simnett* [1968].) Also, electrons from 3 to 12 Mev have been observed for several years [*Cline et al.*, 1964; *Cline and McDonald*, 1968; *Simnett and McDonald*, 1969].

In this paper, we present measurements of the electron spectrum between 17 Mev and 1 Gev. The low end of this energy interval, below 200 Mev, is of particular interest because the observed spectrum of electrons below 12 Mev is not a simple extension of the spectrum above 200 Mev. Delineation of the spectrum in this intermediate interval can provide information about the origin of the cosmic-ray electrons and about solar modulation of cosmic rays. The most recent reports on the energy spectrum in this region were made by *Israel and Vogt* [1968], *Webber* [1968], and *Beuermann et al.* [1969].

Return albedo electrons below several hundred Mev can produce a significant contribution to the flux of electrons incident on the top of the atmosphere and can also contaminate some measurements of relativistic protons. Data regarding the electron albedo are therefore valuable for studies of primary cosmic rays. Accordingly, we have measured the flux of splash albedo electrons between 12 Mev and 1 Gev near Fort Churchill, Manitoba, and return albedo electrons in the same energy interval near Palestine, Texas. No detailed calculation of the intensity or spectrum of the albedo electrons has been published, and only a few observations are available. *Bland* [1965] has made a rough calculation to derive an upper limit to the intensity of return albedo electrons near 45°

[1] Present address: Department of Physics, Washington University, St. Louis, Missouri 63130.

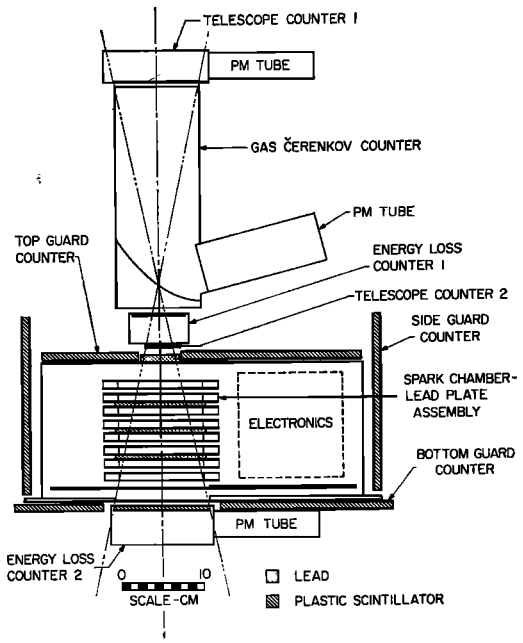

Fig. 1. Cross section of the detector system.

geomagnetic latitude. *Verma* [1967*a*] measured the vertical splash and return albedo near Palestine, Texas, for electrons between 10 and 1100 Mev, with an energy-loss-range counter telescope. *Schmoker and Earl* [1965] observed return albedo electrons between 50 and 150 Mev with a cloud chamber detector near Minneapolis and in Texas. At similar latitudes, *McDonald and Webber* [1959] observed relativistic splash albedo as particles with range greater than 10 g/cm^2 moving backward through an energy-loss Čerenkov detector. No previous measurements of splash albedo electrons near Fort Churchill have been reported.

We also observed return albedo electrons with energy below 100 Mev near Fort Churchill. The high-latitude return albedo measurements are complicated by the diurnal variation of the geomagnetic cutoff, and we postpone discussion of these results to the accompanying paper [*Israel and Vogt*, 1969], which hereafter will be referred to as paper 2.

Instrument

Figure 1 shows a cross section of our detector system. A triple coincidence of telescope counter 1 (T1), telescope counter 2 (T2), and the gas Čerenkov counter (Č) initiates the analysis of an event. The scintillation counters T1 and T2 define an acceptance cone with a geometrical factor of 0.90 ± 0.02 cm^2 ster. The maximum opening angle is 13.2° from the axis.

The Čerenkov counter is filled with sulfur hexafluoride at 2.2 atmospheres absolute pressure (at 25°C), which gives a velocity threshold of 0.9984*c*, corresponding to a kinetic energy of 8.6 Mev for electrons and 15.8 Gev for protons.

The pulse heights from the scintillation counters energy loss 1 and energy loss 2 (ΔE1 and ΔE2) are recorded for each event. Pulse height in ΔE1 corresponding to minimum energy loss establishes that one singly charged particle traversed the telescope. The counter ΔE2 samples the electron shower independently of the spark chamber.

A high-voltage pulse is applied to the spark chamber plates at each T1, T2, Č triple coincidence, and the position of each spark is recorded digitally. A lead plate with a thickness of 11.6 g/cm^2 (2 radiation lengths) is above the chamber, and three lead plates, each 5.8 g/cm^2 thick, are inside the chamber; a pair of chamber gaps is below each lead plate.

The chamber shows no sparks for electrons stopping in the first lead plate, which indicates their short range. For more energetic electrons, the chamber indicates the development of their cascade shower. These electrons can be distinguished from the protons penetrating the lead without a nuclear interaction, because the protons leave a single straight track in the spark chamber.

Most protons that do interact in the detector are eliminated by the guard counters. These counters completely surround the chamber, except for apertures for the allowed particle beam. For each event we record whether a guard counter is triggered in coincidence with the telescope counter. An interacting 16-Gev proton has greater than 90% probability of sending at least one charged particle through a guard counter [*Israel*, 1969]. The guard counters also allow us to eliminate charged particles that enter the detector from outside the acceptance cone but give a triple coincidence by interacting in the lead and sending particles up through the telescope counters. Four of the balloon observations to be discussed (flights C1, C2, C3, and P1) were performed with the

'normal' detector configuration as described above. One other observation (flight C4) was performed with a modified detector configuration. The first modification involved changing the coincidence requirement for analysis from a T1, T2, Č triple coincidence to a double coincidence between T1 and T2, recording separately with each event whether a triple coincidence occurred. Second, we added four 5.8-g/cm²-thick lead plates to the spark chamber in the four spaces between chamber gaps where the normal configuration contained no lead. This modification allowed the measurement of low-energy protons and α particles which stopped or interacted in the spark chamber. It also allowed a lower, although less clean, energy threshold for electron measurements. In this paper, we consider only electron measurements using triple coincidence events.

Balloon Flights

The data reported in this paper are derived from five balloon flights whose pertinent characteristics are summarized in Table 1. Flights C1, C2, and C4, launched from Fort Churchill, Manitoba, provided data on primary electrons. Evidence presented in paper 2 shows that the geomagnetic cutoff rigidity at the location of the detector was below 17 Mv during a 'nighttime' portion of these flights and was near 100 Mv during a 'daytime' portion. Our results for primary electrons below 100 Mev are derived from the nighttime data, and results above 100 Mev are derived from the entire flights. On flight C3, also from Fort Churchill, the detector system was inverted to point toward the nadir and detect upward-moving splash albedo electrons. Throughout flight P1, launched from Palestine, Texas, the vertical geomagnetic cutoff [*Shea et al.*, 1968] at the location of the detector remained above 3.8 Gv, which enabled us to observe return albedo electrons.

Data Analysis

Event selection and energy determination. We attribute to electrons the recorded events that satisfy the following four criteria:

1. A triple coincidence, including the Čerenkov counter, is registered.
2. No guard counter signal accompanies the event.
3. The pulse height from the counter ΔE1 corresponds to energy loss between $0.5I_0$ and $1.7I_0$, where I_0 is the most probable energy loss of a relativistic singly charged particle.
4. Either there is no output from ΔE2, or there is an output from ΔE2 corresponding to energy loss greater than $1.7I_0$ and the spark chamber did not show a single straight track.

These criteria eliminate most of the background due to particles other than electrons, but they also eliminate some electrons. The solid curve in Figure 2 shows the electron detection efficiency as a function of energy.

For electrons with energy between 100 and 1000 Mev we determined the efficiency directly, by using the monoenergetic external electron

TABLE 1. Balloon Flights

Flight number	C1	C2	C3	C4	P1
Launch date, 1967	June 17	July 2	July 9	July 21	April 7
Launch time*	1027	0358	0323	0320	1127
Begin float*	1340	0900	0900	0930	1600
Terminate float*	0330	1745	1925	2115	2155
Floating depth, g/cm²	2.1–3.4	2.0	2.3	2.1	5.2
Sensitive time at float, min	791	504	496	530	346
Orientation	Zenith	Zenith	Nadir	Zenith	Zenith
Configuration†	Normal	Normal	Normal	Modified	Normal
Kp‡	3−	0+	1−	1+	1
Mount Washington neutron monitor§	2274	2244	2285	2317	2260

* Univeral time.
† See section on 'Instrument.'
‡ Mean of three-hour *Kp* indices during float [*Lincoln*, 1968].
§ Mean of hourly count rate during float (J. A. Lockwood, private communication).

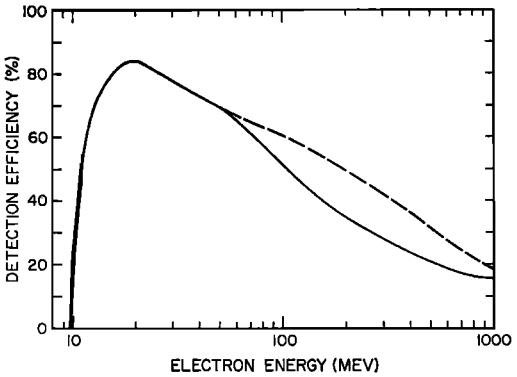

Fig. 2. Electron detection efficiency versus kinetic energy at the top of the detector. Solid curve indicates efficiency with all selection criteria included; dashed curve, efficiency with fourth criterion ignored.

beam at the California Institute of Technology synchrotron. At these energies, the rejection of electrons is principally due to the second criterion, guard counter signals. For lower energies, we derive the efficiency from a combination of measurements and calculations. Below 30 Mev the detection efficiency curve is dominated by the calculated Čerenkov counter response. We estimate that systematic uncertainties in the detection efficiency produce errors of less than 10% of the observed flux at all energies considered.

We divide the selected events into the following categories:

Type 1. Both the spark chamber and ΔE2 register no particle.

Type 2. ΔE2 registers no particle and the total number of sparks in all chamber gaps is one, two, or three.

Type 3. ΔE2 registers no particle, and the total number of sparks is greater than three.

Type 4. ΔE2 registers a pulse height corresponding to energy loss greater than $1.7I_0$.

These four types correspond approximately to electron energies at the top of the detector of 12–50, 50–100, 100–350, and 350–1000 Mev, respectively. We calibrated the detector at the Caltech synchrotron to determine the energy dependence of the probability for producing each type of event. We derive an electron spectrum from the observed number of events of each type and our calibrations with a straightforward iterative unfolding technique [*Israel*, 1969].

Systematic uncertainties. Possible differences between the spark chamber efficiency during flight and during the calibration at the Caltech synchrotron result in a possible error of ±7% in the electron flux between 100 and 350 Mev. In other energy intervals the error from this source is less than 3%.

An additional uncertainty occurs because we could not measure the detection efficiency for electrons above 1 Gev. Thus, an undertermined fraction of the type 4 events is due to these higher-energy electrons. This fraction is small because of the steepness of the differential electron spectrum. Even for a relatively flat spectrum, proportional to E^{-1} (where E is electron energy), the uncertainty in the flux between 350 and 1000 Mev would be less than 15%.

We have considered in detail the possibility of contamination of our electron measurements by protons, pions, and muons [*Israel*, 1969]. The only serious source of error is protons with energy above the gas Čerenkov counter threshold (16 Gev) which interact in the detector system. For flight P1 an upper limit to the proton contamination is 40% of the flux of 350- to 1000-Mev electrons. (This uncertainty is comparable to the statistical uncertainty because we observed only four events in this energy interval.) For the flights C1, C2, and C4 the corresponding error is less than 15%. For flight C3, in which the detector was oriented toward the nadir, the contamination is negligible.

Atmospheric Secondaries

The analysis described above permits us to calculate the spectrum of electrons incident on the detector system. To derive the electron flux incident at the top of the atmosphere, we must subtract the contribution of atmospheric secondary electrons from the observed spectrum.

In the upper 10 g/cm^2 of the atmosphere, the principal source of secondary electrons at energies $\gtrsim$20 Mev is the decay of charged pions that originate in interactions of primary cosmic-ray nuclei with air nuclei. The resulting secondary electron spectrum has been calculated from the known primary cosmic-ray spectrum at solar minimum and the pion production cross sections by *Perola and Scarsi* [1966] and

by *Verma* [1967*b*]. The calculated electron spectra at 2-g/cm² atmospheric depth are shown in Figure 3. Also shown is the spectrum of knock-on electrons (K. Beuermann, to be published) and the combined spectra formed by adding the knock-on electrons to the electrons originating in interactions. At energies $\lesssim$100 Mev the two independently calculated spectra differ by a factor of 2 to 3, although both authors claim an uncertainty of less than 25%. Between 200 and 1000 Mev, the two are in good agreement.

The importance of the secondary electron contribution at these energies is clear when we consider the variation of electron flux with atmospheric depth (Figure 4). In flights C1, C2, and C4, the observed rate of type 1 events (electrons of approximately 12 to 50 Mev) decreases almost linearly with atmospheric depth indicating that even at 2 g/cm² a large fraction of the observed electrons are atmospheric secondaries. Also plotted in Figure 4 (curves 1 and 2) are the expected event rates derived by folding the type 1 detection probability with the secondary electron spectra calculated by Perola and Scarsi and by Verma. We include the knock-on electron contribution in these curves. We also make an approximate correction for the difference between the primary proton flux assumed in the calculations and the proton flux at the time of our flights. This correction gives a 15% decrease for the spectrum based on the calculation of Perola and Scarsi and a 5% decrease for that of Verma.

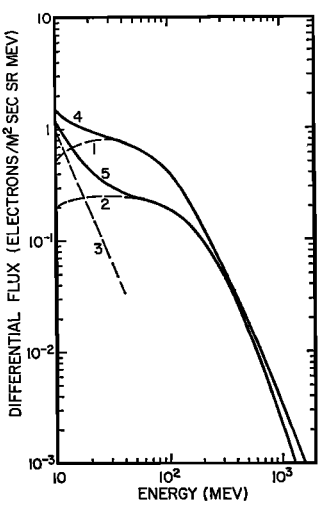

Fig. 3. Kinetic energy spectrum of atmospheric secondary electrons at 2-g/cm² atmospheric depth. Curve 1 represents electrons from nuclear interactions [*Perola and Scarsi*, 1966]; curve 2, electrons from nuclear interactions [*Verma*, 1967*b*]; curve 3, knock-on electrons; curve 4, sum of curves 1 and 3; curve 5, sum of curves 2 and 3.

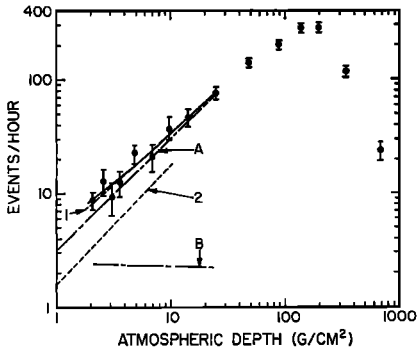

Fig. 4. Rate of type 1 events versus atmospheric depth. Data points are combined results of data gathered during ascent of flights C1, C2, and C4 and data gathered during 'night' portion of float on flights C2 and C4 (See paper 2 for distinction between 'day' and 'night' data. Ascent of all flights occurred at 'night.') Curve 1 represents count rate derived from *Perola and Scarsi* [1966] with addition of knock-on electrons; curve 2, count rate derived from Verma [1967*b*] with addition of knock-on electrons; solid line, least-squares fit to data, assuming $s(d) = d$; curve A, secondary contribution to solid line; curve B, Primary contribution to solid line.

Because the two calculated secondary electron fluxes are in disagreement at low energies, we make an independent estimate, based on our data of Figure 4 as follows. We take the altitude dependence of the total flux of type 1 electrons $J(d)$ to be of the form

$$J(d) = as(d) + bp(d) \qquad (1)$$

where d is atmospheric depth, the function $s(d)$ describes the depth dependence of the flux of secondary electrons, the function $p(d)$ describes the depth dependence of the flux due to primary electrons, and the coefficients a and b are parameters that we determine by a least-squares fit to the nine data points from 2 to 25 g/cm².

The solid curve in Figure 4 is the least-squares fit for $J(d)$ based on the following assumptions:

1. $s(d)$ varies linearly with depth, i.e. the depth dependence of the calculated curve 2.
2. $p(d)$ is calculated by assuming a primary

electron spectrum of the form E^{-n} with $n = 0.5$. The flux of primary electrons in the energy interval corresponding to type 1 events varies with depth as the incident electrons lose energy in penetrating the atmosphere.

Curves A and B indicate the secondary and primary contributions, respectively, to the least-squares fit. The solid curve, which is the sum of A and B, fits the data with a χ^2 of 2.9. The primary contribution at 2.1 g/cm^2 resulting from this fit is 2.4 ± 1.5 events/hr, approximately one-fourth of the observed events. This result is not sensitive to the choice of n, the exponent of the primary energy spectrum. It differs from this value by less than 10% for any value of n between 0 and 2.

On the other hand, the results of the fit are very sensitive to the assumed depth dependence of the secondary flux. If we take $s(d) = d^{0.9}$ (in agreement with the depth dependence of curve 1), the least-squares fit gives a primary electron contribution of 0.4 ± 1.6 event/hr, consistent with zero. In this case, the secondary electron contribution to the least-squares fit agrees with curve 1 within 5%, well within the 20% stated accuracy of the calculation from which curve 1 is derived.

If we take the secondary depth dependence as $s(d) = d^m$ and allow m to vary as a third parameter, we find the minimum χ^2, 2.5 for $m = 0.85$; in this case the primary electrons give −0.8 ± 1.7 event/hr, still consistent with zero. We do not claim to have established a value of m from this analysis, but only point out that any reasonable least-squares fit to our data is consistent with a very small contribution of primary electrons.

This analysis leads us to two conclusions about electrons in the interval 12 to 50 Mev. First, our observations are in good agreement with the calculations of Perola and Scarsi and in disagreement with those of Verma. The contribution of atmospheric secondaries to our observed data falls within 20% of curve 1 (derived from Perola and Scarsi) whether we assume the secondary electron flux to vary linearly with depth or as slowly as $d^{0.85}$. We cannot reconcile our observations with a secondary contribution near curve 2. Second, we conclude that our results are consistent with the entire observed flux's being atmospheric secondaries. As an upper limit to the primary contribution to type 1 events, we take the result of the least-squares fit assuming linear growth of secondaries, 2.4 ± 1.5 events/hr.

For higher-energy electrons our count rate is so low that measurements of the rate during the balloon ascent have very large statistical uncertainty, precluding useful least-squares fitting. We note, however, that at energies above 200 Mev the two calculations agree with one another as well as agreeing with the secondary flux derived from measurements of both *L'Heureux* [1967] and *Beedle and Webber* [1968]. Therefore, we shall calculate the spectrum of the total flux at the detector and then subtract the spectrum of atmospheric secondaries based on the calculations of Perola and Scarsi in order to derive the primary flux. These spectra are presented below.

We note that in the 12- to 50-Mev interval *Beedle and Webber* [1968] in 1966 find a flux of atmospheric secondary electrons lower by approximately a factor of 2 than our 1967 value. This difference can be traced back to a similar difference in the total observed flux of electrons at 10- to 20-g/cm^2 atmospheric depth. The difference cannot be explained as a time variation because the flux of cosmic-ray nuclei, which produce the secondary electrons, was lower in 1967 than in 1966. Thus, there is a clear disagreement between the two groups' corrections for low-energy secondary electrons.

Primary Electrons

Results. In this discussion of our primary electron observations, we accept the explanation of the diurnal flux variation described in paper 2. For the types of electron events that display a diurnal variation, types 1 and 2, we shall use only the nighttime data. For the events of type 3 and 4 (higher electron energies), which display no significant diurnal variation, we shall use data gathered over the entire float period of each flight. We apply the analysis described above to derive the flux of electrons observed at the detector, including primaries and atmospheric secondaries. The results are listed in lines 2, 3, and 4 of Table 2. The float altitudes of flights C2 and C4 agreed within 0.1 g/cm^2, and the observed electron fluxes in the two flights are in close agreement. Therefore, the results of these two flights have been combined, yielding

TABLE 2. Primary Electron Flux (electrons/m² sec ster)

Errors listed include 1σ statistical uncertainty plus possible systematic error. Upper limits represent 2σ statistical uncertainty, plus possible systematic error.

1.	Energy interval at detector, Mev	12–50	50–100	100–350	350–1000
2.	Total flux at detector, flight C1	39 ± 12	31 ± 11	38 ± 15	23 ± 11
3.	Flight C2	27 ± 10	17 ± 9	25 ± 12	26 ± 15
4.	Flight C4	31 ± 10	15 ± 7	20 ± 8	22 ± 13
5.	Flights C2 and C4	29 ± 8	16 ± 7	23 ± 10	24 ± 12
6.	Atmospheric secondaries at 2 g/cm² (C2 & C4)	28 ± 6	23 ± 5	31 ± 6	8 ± 2
7.	Primary electrons, flights C2 and C4				16 ± 14
8.	Upper limit to primary electrons, flights C2 and C4	20	9	13	(35)
9.	Atmospheric secondaries (mean during C1)*	41 ± 9	33 ± 7	37 ± 7	10 ± 2
10.	Upper limit to primary electrons, flight C1	21	23	20	(31)
11.	Energy interval at top of atmosphere, Mev	17–57	57–112	112–374	374–1060

* During flight C1, atmospheric depth varied between 2.1 and 3.4 g/cm².

the fluxes tabulated in line 5. In Figure 5 we plot the differential energy spectra derived from these data. Also plotted in this figure is the calculated spectrum of atmospheric secondaries at the float altitude of flights C2 and C4.

In line 6 of Table 2 we list the atmospheric secondary fluxes for flights C2 and C4. We note that below 350 Mev our total observed flux is consistent with the flux expected from atmospheric secondaries only; i.e., our results below 350 Mev are consistent with the complete absence of primary electrons. In line 8 of Table 2 we list upper limits to the primary electron fluxes. Similar subtraction of atmospheric secondaries for flight C1, which had a lower average float altitude, are indicated in lines 9 and 10. The last line of Table 2 gives the energy intervals at the top of the atmosphere to which the calculated primary fluxes correspond. This adjustment of energy intervals takes into account the energy loss of primary electrons in penetrating 2.1 g/cm² of air, by using the calculated values of electron range in air, including energy loss by both ionization and radiation [*Berger and Seltzer*, 1964].

The observed flux of electrons between 50 and 350 Mev appears to be higher on flight C1 than on flights C2 and C4, even after accounting for the difference in atmospheric secondaries. The deviation lies, however, at the edge of the

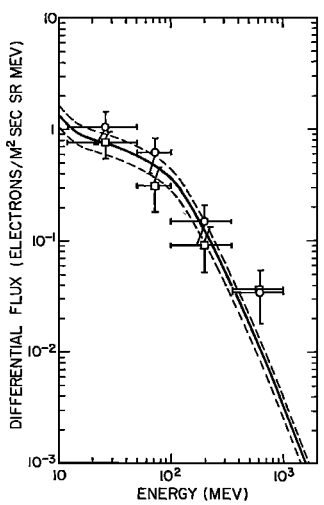

Fig. 5. Differential kinetic energy spectrum of downward-moving electrons. Data points indicate total observed electron flux at detector during float. For the types of events displaying a diurnal variation only nighttime data are used. (Vertical error bars indicate combined statistical and systematic uncertainty.) Circles indicate flight C1, 2.1 to 3.4 g/cm²; squares, flights C2 and C4, 2.1 g/cm². Solid curve indicates atmospheric secondaries at depth of flights C2 and C4 based on calculations of Perola and Scarsi. Adjustments are included for knock-on electrons and for the difference between the proton flux at the time of our flights and that for which the calculations were made. Dashed curves indicate ±20% uncertainty band about the calculated secondary spectrum.

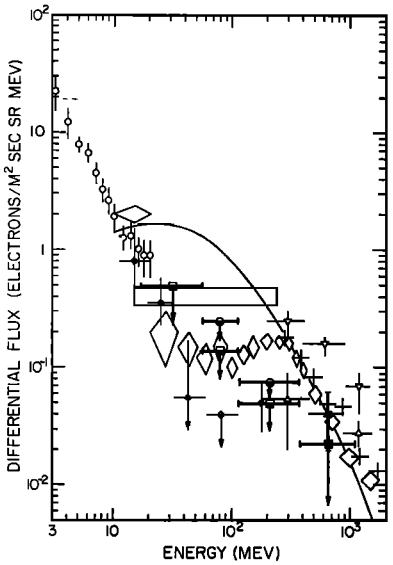

Fig. 6. Differential kinetic energy spectrum of primary electrons. Solid and semi-solid squares and circles represent results from this experiment, June and July 1967 (semi-solid symbols being upper limits). Squares indicate flights C2 and C4; circles, flight C1, where different from C2 and C4; open diamonds, results from *Webber* [1968] for July 1966; crosses, *L'Heureux and Meyer* [1968] for June 1966; large rectangle, *Jokipii et al.* [1967] for June 1966; open triangles (point up), *Fanselow* [1968] for 1965; open triangles (point down), *Simnett* [1968] for 1967; closed diamonds, *Beuermann et al.* [1969] for July 1968; open circles, *Simnett and McDonald* [1969] 1967. Solid curve is calculated interstellar spectrum of galactic secondary electrons [*Ramaty and Lingenfelter*, 1968].

experimental uncertainty. More precise results would be required to confirm a short-term flux variation.

In Figure 6 we plot the differential fluxes derived from our data and the results of other recent electron measurements. In plotting results of other observers, we omit any data point that includes electrons with energy below 110 Mev unless it is derived from nighttime observations only or from spacecraft observations outside the magnetosphere.

Discussion. Above 100 Mev, the flux of primary electrons that we observed in 1967 is significantly lower than the 1966 flux reported by *Webber* [1968] and by *L'Heureux and Meyer* [1968]. Between 112 and 374 Mev the upper limit to the primary flux of our flights C2 and C4 is a factor of 3 below the flux reported by Webber. Between 374 Mev and 1060 Mev our best estimate of the flux is nearly a factor of 2 below that of Webber and of L'Heureux and Meyer. On the other hand, our results are in agreement with the 1965 observations of *Fanselow* [1968], whereas the 1967 observations of *Simnett* [1968] are significantly higher than those of any other observer. The difference between our 1967 measurements and other 1966 measurements may be attributed to solar modulation of the electron flux. However, the differences among the various observers cited above indicate the possibility of systematic errors. Thus, there would be considerable uncertainty involved in deriving quantitative information on modulation by comparing our data with theirs.

Figure 6 shows that below 112 Mev our upper limits for the primary flux are consistent with the values reported by Webber and are also consistent with the values of *Beuermann et al.* [1969]. Our results disagree with the values of Jokipii et al., but this difference lies primarily in the correction for atmospheric secondaries. They used the atmospheric secondary corrections calculated by *Verma* [1967*b*], which we find yield too low a flux of secondary electrons below 100 Mev.

Finally, a comparison of our measured upper limits of the 1967 primary electron flux with calculated interstellar electron spectra allows us to set a lower limit to the total solar modulation of cosmic-ray electrons. The solid curve in Figure 6 represents the calculated interstellar spectrum of secondary electrons produced by collisions of cosmic-ray nuclei with interstellar matter [*Ramaty and Lingenfelter*, 1968]. Under the assumptions used in the calculation, this curve must be treated as a lower limit to the interstellar electron spectrum because of additional electrons from other sources. Since the upper limit to our electron flux below 300 Mev lies a factor of 3 below this curve, we conclude that there must be significant modulation of these low-energy electrons, a reduction in flux by at least a factor of 3. (If the absolute modulation were proved smaller than this, our data would imply that some of the galactic parameters used in Ramaty and Lingenfelter's calculation were seriously in error.) This conclusion is consistent with the more precise results of *Beuermann*

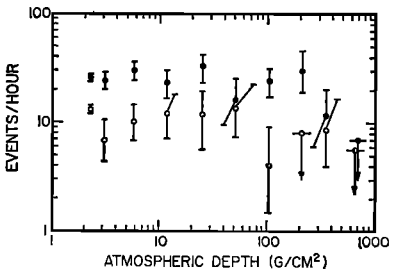

Fig. 7. Event rate of upward-moving electrons versus atmospheric depth. Solid circles represent type 1 events; open circles, type 2 and 3 events.

et al. [1969]. Because their detector system distinguished positrons from negatrons, their comparison of observed and calculated positron spectra allowed conclusions to be made on the absolute solar modulation in 1968.

Albedo Electrons

Splash albedo near Fort Churchill. During the flight of July 9, 1967, we observed upward-moving electrons. Figure 7 displays the altitude dependence of the rate of type 1 events and of types 2 and 3. The data points at 2.3-g/cm² atmospheric depth represent averages over the 10.4-hour float period. The other data were gathered during the 5.6-hour ascent.

It is apparent from Figure 7 that there is little or no altitude variation of the splash albedo between 2.3 and 50 or 100 g/cm². We shall therefore assume that the electron energy spectrum we observed at the detector at 2.3 g/cm² is the same as the spectrum at the top of the atmosphere. The number of events of each type observed during the float period of flight C3 is shown in Table 3. Applying the analysis described above, we derive the flux values shown in Table 4. The solid circles in Figure 8 indicate the differential energy spectrum derived from these measurements. The error limits quoted include statistical and systematic uncertainties.

TABLE 3. Number of Electron Events Observed

Flight date	July 9, 1967	April 7, 1967
Launch location	Fort Churchill	Palestine
Detector orientation	Nadir	Zenith
Event type 1	212	152
Event type 2	86	42
Event type 3	21	15
Event type 4	3	5
Sensitive time, min	496	346

To simplify comparison between our results and the results of other experimenters, Table 4 gives our fluxes summed over various energy intervals. In Table 5 we summarize the splash albedo results of other observers. We note that in all energy intervals our measured flux lies significantly below the flux quoted by Verma. On the other hand, our flux above 50 Mev is in reasonable agreement with that of McDonald and Webber and our flux above 100 Mev is consistent with the upper limit derived by Deney et al.

Return albedo near Palestine, Texas. The number of events of each type observed during the float period of the April 7 flight is listed in Table 3. In Table 6, line 2, we present the electron fluxes in various energy intervals derived from these events. The corresponding differential energy spectrum is plotted as solid points in Figure 9. Also shown, in line 3 of Table 6, is the flux of atmospheric secondary electrons expected at 5 g/cm² near Palestine. The only energy interval in which we observe a clear excess over the secondaries is 12 to 50 Mev, where the return albedo contribution is 60 ± 26 electrons/m² sec ster. For the other intervals line 5 of Table 6 gives upper limits to the return albedo flux. These limits represent two standard deviations of statistical uncertainties, plus the systematic uncertainty. In line 6 we have tabulated the energy intervals at the top of the atmosphere to which the calculated primary fluxes correspond.

TABLE 4. Splash Albedo Electrons: Results of This Experiment, Fort Churchill, Manitoba

Energy interval, Mev	12–50	50–100	100–350	350–1000
Flux, electrons/m² sec ster	94 ± 16	47 ± 11	27 ± 9	2_{-2}^{+4}
Combined flux, 12–100 Mev	141 ± 24			
100–1000 Mev			29 ± 10	
Flux between 50 and 1000 Mev		76 ± 16		

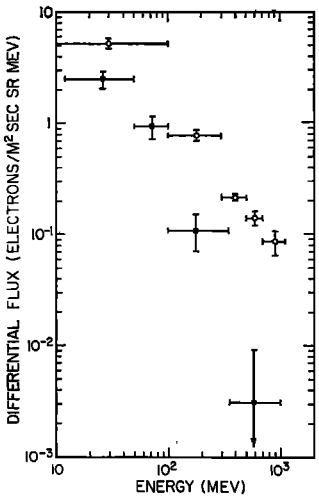

Fig. 8. Differential kinetic energy spectrum of splash albedo electrons. Solid circles represent present experiment, Fort Churchill. Canada; open circles, experiment of *Verma* [1967*a*], Palestine, Texas.

In the last line of Table 6 we list for comparison the splash albedo fluxes from the Fort Churchill flight in these higher-energy intervals. We derived these flux values from those of Table 4 by using the observed differential splash albedo spectrum from Figure 8. For further comparison, Table 7 lists results from return albedo measurements by other observers. We have tabulated the total observed flux, including return albedo and atmospheric secondaries. These results are also plotted in Figure 9.

Discussion. We first compare our return albedo measurement near Palestine, Texas, with Verma's. His measurements were made on two balloon flights also launched at Palestine. There is a significant disagreement between Verma's results and ours, especially above 100 Mev. We note that this disagreement appears already in the total observed flux at the detector, before correction for atmospheric secondaries. Since the flux of atmospheric secondaries at the float altitude of his flights (4.0 g/cm²) is within 25% of the value at the altitude of our flight (5.2 g/cm²), although our total fluxes differ by approximately a factor of 3 or more, the comparison of total fluxes is valid.

The 2-year time difference between Verma's flights and ours can account for only a small part of the difference in results. From 1965, when his data were taken, to the time of our flights the Mount Washington neutron-monitor count rate decreased by 9%. The corresponding decrease in the flux of cosmic-ray protons and helium nuclei above the geomagnetic cutoff at Palestine (4.5 Gv) is 10%. (This number is based on regression curves of data from the last solar cycle [*Webber*, 1967].) The corresponding decrease in the albedo intensity must be $\leq 10\%$. This upper limit follows because the change in primary flux is largest at the lowest energy, whereas the electron production by electromagnetic cascades is larger at higher primary energies. Similarly, the change in flux of atmospheric secondaries must be $\leq 10\%$. A 10% reduction in Verma's flux between 10 and 100 Mev would bring it within the quoted error of our result. For energies above 100 Mev, how-

TABLE 5. Splash Albedo Electrons: Results of Other Experiments

Reference	Date	Location	Cutoff,* Gv	Energy Interval, Mev	Flux, electrons/m² sec ster
Verma [1967*a*]	1965	Palestine, Texas	4.5	10–100	467 ± 48
				100–300	134 ± 15
				300–1100	108 ± 18
McDonald and Webber [1959]	1956	Iowa City	1.8	≳40†	84 ± 8
	1956	Minneapolis	1.4	≳40†	89 ± 8
Deney et al. [1968]	1967	Palestine, Texas	4.5	>100	<100

* *Shea et al.* [1968]

† These electrons were identified only as having range greater than 10 g/cm². The corresponding energy is estimated from our own detector calibration at the Caltech synchrotron.

TABLE 6. Return Albedo: Results of This Experiment, Palestine, Texas
Fluxes in units of electrons/m² sec ster.

1.	Energy interval at detector, Mev	12–50	50–100	100–350	350–1000
2.	Total observed flux at 5.2 g/cm²	95 ± 19	29 ± 9	31 ± 14	8_{-4}^{+8}
3.	Calculated flux of atmospheric secondaries	35 ± 7	26 ± 5	50 ± 10	17 ± 3
4.	Return albedo flux	60 ± 26			
5.	Return albedo flux upper limit (2σ)	(96)	22	12	6
6.	Energy interval at the top of the atmosphere, Mev	25–65	65–131	131–411	411–1149
7.	Corresponding splash albedo flux, near Fort Churchill	63 ± 11	44 ± 10	13 ± 4	<5

ever, the difference between his results and ours remains significant.

This difference indicates the possibility of a systematic error in either Verma's or our measurements. We have considered possible sources of error in our results, including the possibility of error in the determination of our detection efficiency (Figure 2). Furthermore, in the energy interval between 350 and 1000 Mev our return albedo flux is at least a factor of 4 below Verma's, although in the same energy interval our primary flux measurements at Churchill in 1967 (before correcting for atmospheric secondaries) are less than a factor of 2 below corresponding published measurements for 1966. This factor may be due to modulation.

Bland [1965] has published a rough calculation of the return albedo flux at 4-g/cm² atmospheric depth, 45° geomagnetic latitude. His result, as an upper limit to the flux of electrons above 100 Mev, is 14 electrons/m² sec ster. If the electrons are isotropic over the upper hemisphere, this would correspond to 2.2 electrons/m² sec ster. This flux is consistent with our upper limit, 18 electrons/m² sec ster after subtracting atmospheric secondaries. Verma, on the other hand, derives a corresponding value of 94 ± 25 electrons/m² sec ster.

We next consider our measurement of the splash albedo near Fort Churchill. Both the location and the time of the measurement by McDonald and Webber near Minneapolis enable us to compare their result with ours. The geomagnetic cutoff at Minneapolis, 1.4 Gv, corresponds to a proton energy of 750 Mev. The difference between this cutoff and that near Churchill, $\lesssim$100 Mv, is not significant for the production of albedo electrons. At the time of the Minneapolis flight, the Mount Washington neutron monitor count rate was 2302, 0.7% higher than during our flight. This corresponds to a 6% difference in the primary proton flux [*Webber*, 1967] and less than 6% difference in the albedo flux. The albedo flux measured by

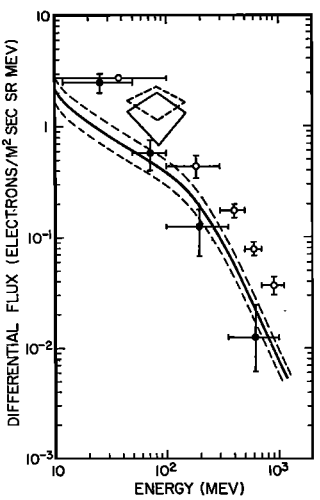

Fig. 9. Differential kinetic energy spectrum of downward-moving electrons below geomagnetic cutoff. Data points indicate total observed flux, including return albedo and atmospheric secondaries. Solid curve indicates calculated spectrum of atmospheric secondaries at 5-g/cm² atmospheric depth. Dashed curves indicate quoted uncertainty in this calculated spectrum (±20%). Solid circles represent present experiment, Palestine, Texas, 5 g/cm²; open circles, *Verma* [1967*a*], Palestine, Texas. 4 g/cm²; solid-line diamond, *Schmoker and Earl* [1965], San Angelo, Texas, 6 g/cm²; dashed-line diamond, *Schmoker and Earl* [1965], Minneapolis, Minnesota, 4–5 g/cm².

TABLE 7. Return Albedo: Results from Other Experiments

Reference	Date	Location	Cutoff, Gv	Atomspheric Depth, g/cm²	Energy Interval, Mev	Total Observed Flux at Detector, electrons/m² sec ster
Verma [1967*a*]	1965	Palestine, Texas	4.5	4.0	10–100	162 ± 16
					100–300	90 ± 30
					300–1100	68 ± 10
Schmoker and	1962	San Angelo, Texas	5.0	6	45–150	140 ± 70
Earl [1965]	1962 and 63	Minneapolis	1.4	4–5	45–150	180 ± 60

McDonald and Webber, 84 ± 8 electrons/m² sec ster, is in good agreement with our corresponding flux, 76 ± 17 electrons/m² sec ster, above 50 Mev.

We cannot attempt to draw any conclusion about the latitude dependence of the splash albedo from comparison of our results with Verma's because of the apparent instrumental differences previously noted. We shall, however, compare our own return albedo measurement near Palestine with our splash albedo observation near Churchill (lines 4–7 of Table 6). The intensities of the splash and the return albedo at rigidities below the local geomagnetic cutoff are expected to be equal at any point at the top of the atmosphere, provided that the magnetic field strength at the given point is the same as at the conjugate point in the other hemisphere. This equality follows from the splash origin of the return albedo and the fact that the primary cosmic-ray flux at a given geomagnetic latitude in the northern and southern hemispheres is the same. Although the splash and return intensities, integrated over all directions, should be the same, the *vertical* splash albedo flux may be lower than the *vertical* return albedo flux. The dominant source of splash albedo electrons is likely to be cascade showers from interactions of primary cosmic rays entering the atmosphere at grazing incidence [*Bland*, 1965]. Such showers tend to be collimated in the direction of the incident primary particle, so that we expect the splash albedo to be most intense at large zenith angles. *Treiman* [1953] has pointed out that the return albedo will tend to be less anisotropic than the splash albedo. As a result, we expect the vertical return albedo flux to be an upper limit to the vertical splash albedo at the same location.

We note that this expected relationship between the splash and return albedo fluxes has not been extensively tested. The only previously published observation of both splash and return albedo electrons with the same instrument near the same location is that of *Verma* [1967]. The observed difference between the splash and albedo fluxes was not considered significant. Also, we show in paper 2 that our observations near Fort Churchill are consistent with equality between the splash and return albedo fluxes below 100 Mev. We feel, however, that uncertainty in the precise value of the 'daytime' geomagnetic cutoff at the location of the detector introduces significant uncertainty in the interpretation of any return albedo measurement near Fort Churchill.

For the purpose of discussing our results (Table 6) we assume that the return albedo flux that we observed near Palestine is indeed an upper limit to the splash albedo flux at the same location. Between 65 and 131 Mev the Churchill splash albedo exceeds the Palestine return albedo by at least 50%, and between 25 and 65 Mev the return and splash albedo fluxes are in agreement. We cannot explain the apparent difference between these two adjacent energy intervals; however, we note that our results are consistent with a 50% flux excess at Churchill over the entire observed energy interval. Such an excess at Churchill would indicate that primary cosmic rays below the 4.5-Gv cutoff of Palestine contribute significantly to the production of splash albedo electrons. Since the flux of primaries below 4.5 Gv displays significant modulation over the solar cycle, we expect

that the splash albedo electron flux at high latitudes will exhibit similar long-term variations.

Acknowledgments. I am indebted to Professor Rochus Vogt, who originally suggested this experiment and offered valuable guidance and support during all phases of the project. I am also grateful to Dr. Klaus Beuermann, Mr. Carl Rice, and Professor Edward Stone for numerous helpful discussions.

This work was supported by the National Aeronautics and Space Administration under grant NGL-05-002-007.

References

Beedle, R. E., and W. R. Webber, Measurements of cosmic-ray electrons in the energy range 4 Mev to 6 bev at 2 g/cm² atmospheric at Ft. Churchill, *Can. J. Phys., 46,* S1014, 1968.

Berger, M. J., and S. M. Seltzer, Tables of energy losses and ranges of electrons and positrons, *NASA Rept. SP-3012,* 1964.

Beuermann, K. P., C. J. Rice, E. C. Stone, and R. E. Vogt, Cosmic-ray negatron and positron spectra between 12 and 220 Mev, *Phys. Rev. Letters, 22,* 412, 1969.

Bland, C. J., An estimate of the contribution from reentrant albedo to the measurement of primary electrons, *Space Res., 5,* 618, 1965.

Cline, T. L., G. H. Ludwig, and F. B. McDonald, Detection of interplanetary 3–12 Mev electrons, *Phys. Rev. Letters, 13,* 786, 1964.

Cline, T. L., and F. B. McDonald, Interplanetary and solar electrons of energy 3–12 Mev, *Can. J. Phys., 46,* S761, 1968.

Deney, C. L., M. F. Kaplan, and P. W. Lommen, Integral fluxes of primary cosmic rays at Palestine, Texas, and Fort Churchill, Canada, near solar minimum (abstract), *Bull. Am. Phys. Soc., 13,* 63, 1968.

Earl, J. A. Cloud chamber observations of primary cosmic-ray electrons, *Phys. Rev. Letters, 6,* 125, 1961.

Fanselow, J. L., The primary cosmic-ray electron spectrum between 0.09 and 8.4 bev in 1965, *Astrophys. J., 152,* 783, 1968.

Israel, M. H., Primary cosmic-ray electrons and albedo electrons in 1967 at energies between 12 and 1000 Mev, Ph.D. thesis, California Institute of Technology, Pasadena, 1969.

Israel, M. H., and R. E. Vogt, Flux of cosmic-ray electrons between 17 and 63 Mev, *Phys. Rev. Letters, 20,* 1053, 1968.

Israel, M. H., and R. E. Vogt, Characteristics of the diurnally varying electron flux near the polar cap, *J. Geophys. Res., 74,* this issue, 1969.

Jokipii, J. R., J. L'Heureux, and P. Meyer, Diurnal intensity variation of low-energy electrons observed near the polar cap, *J. Geophys. Res., 72,* 4375, 1967.

L'Heureux, J., The primary cosmic-ray electron spectrum near solar minimum, *Astrophys. J., 148,* 399, 1967.

L'Heureux, J., and P. Meyer, The primary cosmic-ray electron spectrum in the energy range from 300 Mev to 4 bev from 1964 to 1966, *Can. J. Phys., 46,* S892, 1968.

Lincoln, J. V., Geomagnetic and solar data, *J. Geophys. Res., 73,* 3094, 1968.

McDonald, F. B., and W. R. Webber, Proton component of the primary cosmic radiation, *Phys. Rev., 115,* 194, 1959.

Meyer, P., and R. E. Vogt, Electrons in the primary cosmic radiation, *Phys. Rev. Letters, 6,* 193, 1961.

Perola, G. C., and L. Scarsi, Flux and energy spectrum of secondary electrons in the upper atmosphere, *Nuovo Cimento, 46,* 718, 1966.

Ramaty, R., and R. E. Lingenfelter, Solar modulation and the galactic intensity of cosmic-ray positrons and negatrons, *Phys. Rev. Letters, 20,* 120, 1968.

Schmoker, J. W., and J. A. Earl, Magnetic-cloud-chamber observations of low-energy cosmic-ray electrons, *Phys. Rev., 138,* B 300, 1965.

Shea, M. A., D. F. Smart, and J. R. McCall, A five degree by fifteen degree world grid of trajectory-determined vertical cutoff rigidities, *Can. J. Phys., 46,* S1098, 1968.

Simnett, G. M., The intensity and time variation of primary cosmic-ray electrons, *Goddard Space Flight Center Preprint X-611-68-108,* 1968.

Simnett, G. M., and F. B. McDonald, Observations of cosmic-ray electrons between 2.7 and 21.5 Mev, *Astrophys. J.,* 1969.

Treiman, S. B., The cosmic-ray albedo, *Phys. Rev., 91,* 957, 1953.

Verma, S. D., Measurement of the charged splash and re-entrant albedo of the cosmic radiation, *J. Geophys. Res., 72,* 915, 1967*a*.

Verma, S. D., A calculation of the flux and energy spectrum of secondary electrons at high altitudes in the atmosphere, *Proc. Indian Acad. Sci., 66,* 125, 1967*b*.

Webber, W. R., The spectrum and charge composition of the primary cosmic radiation, *Handbuch der Physik, 46,* part 2, 181, 1967.

Webber, W. R., Diurnal variation of the intensity and energy spectrum of low-energy electrons incident at Fort Churchill, Canada, *J. Geophys. Res., 73,* 4905, 1968.

(Received December 18, 1968;
revised June 5, 1969.)